

## Supporting Information

### **Microcavity-Free Broadband Light Outcoupling Enhancement in Flexible Organic Light-Emitting Diodes with Nanostructured Transparent Metal-Dielectric Composite Electrodes**

*Lu-Hai Xu,<sup>†</sup> Qing-Dong Ou,<sup>†</sup> Yan-Qing Li,\* Yi-Bo Zhang, Xin-Dong Zhao, Heng-Yang Xiang, Jing-De Chen, Lei Zhou, Shuit-Tong Lee, and Jian-Xin Tang\**

Institute of Functional Nano & Soft Materials (FUNSOM), Collaborative Innovation Center of Suzhou Nano Science and Technology, Jiangsu Key Laboratory for Carbon-Based Functional Materials & Devices, Soochow University, Suzhou 215123, China

<sup>†</sup> These authors contributed equally to this work.

\* Corresponding authors. E-mail addresses: [jxtang@suda.edu.cn](mailto:jxtang@suda.edu.cn) (J.X. Tang), [yqli@suda.edu.cn](mailto:yqli@suda.edu.cn) (Y.Q. Li).

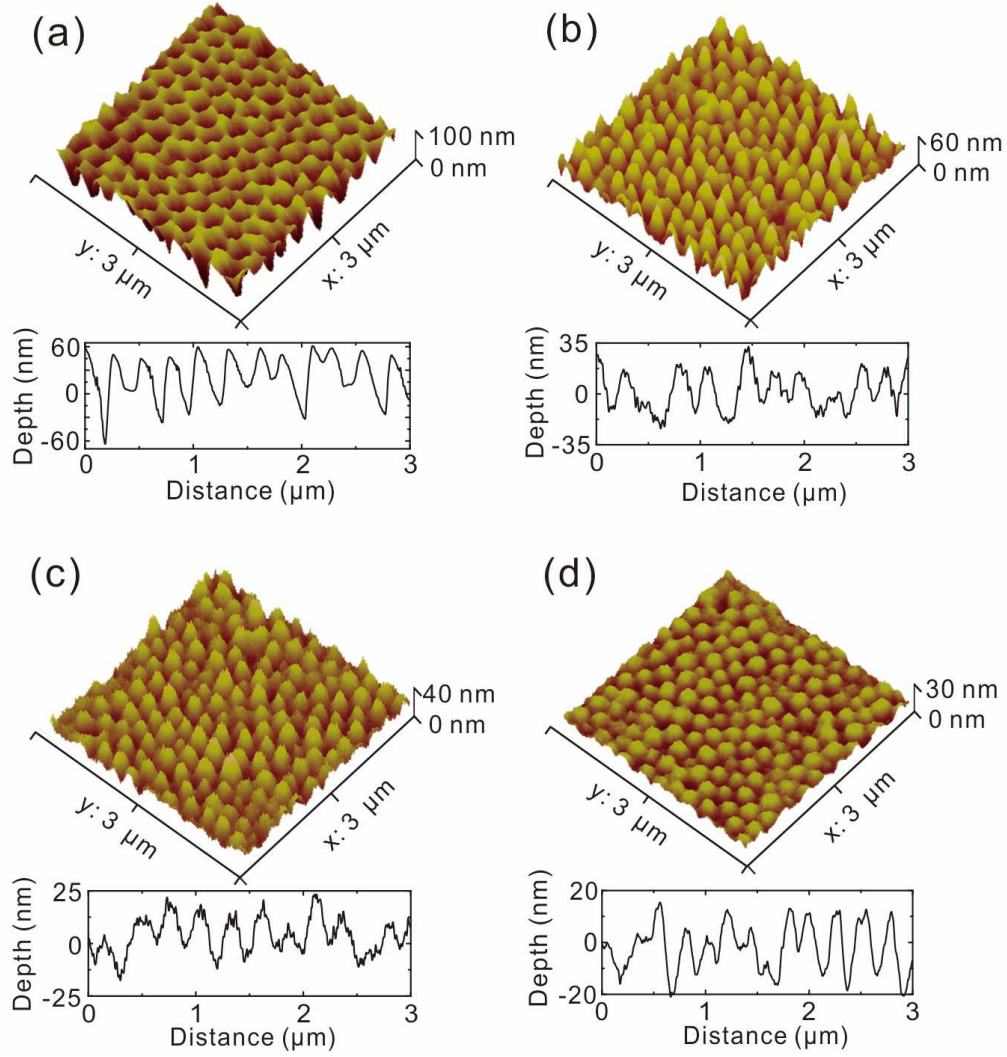


**Figure S1.** Topographic surface images and surface profiles taken by AFM measurements during sequential layer deposition onto plastic substrate. (a) The PFPE mold with a quasi-random nanostructure, showing a period of  $\sim 250$  nm, a groove depth of  $\sim 100$  nm, and a fill factor of  $\sim 0.6$ . AFM images of (b) imprinted UV-resin layer on plastic substrate, (c) subsequently deposited organic layers and (d) top metal electrode on NMDCE, revealing the conformal coating of the corrugated structures over all layers in the device.

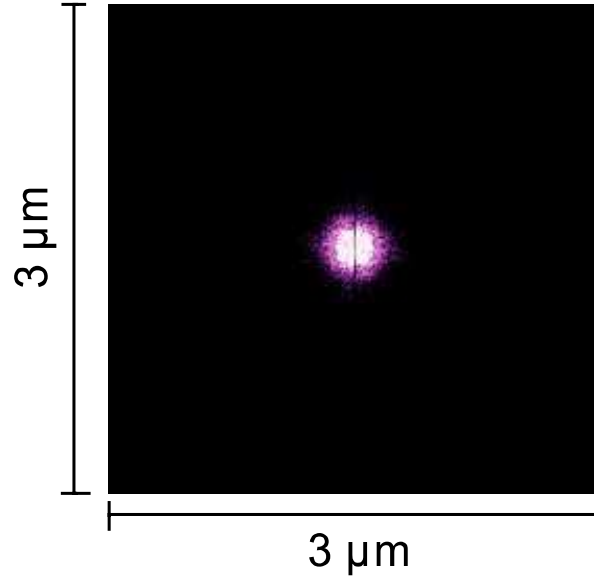


**Figure S2.** Fast Fourier transform (FFT) pattern of nanostructured UV-resin layer as shown in Figure S1b. Fourier energy concentrated into a circular region implies a broadband response of the nanostructures as a quasi-Lambertian scatter.

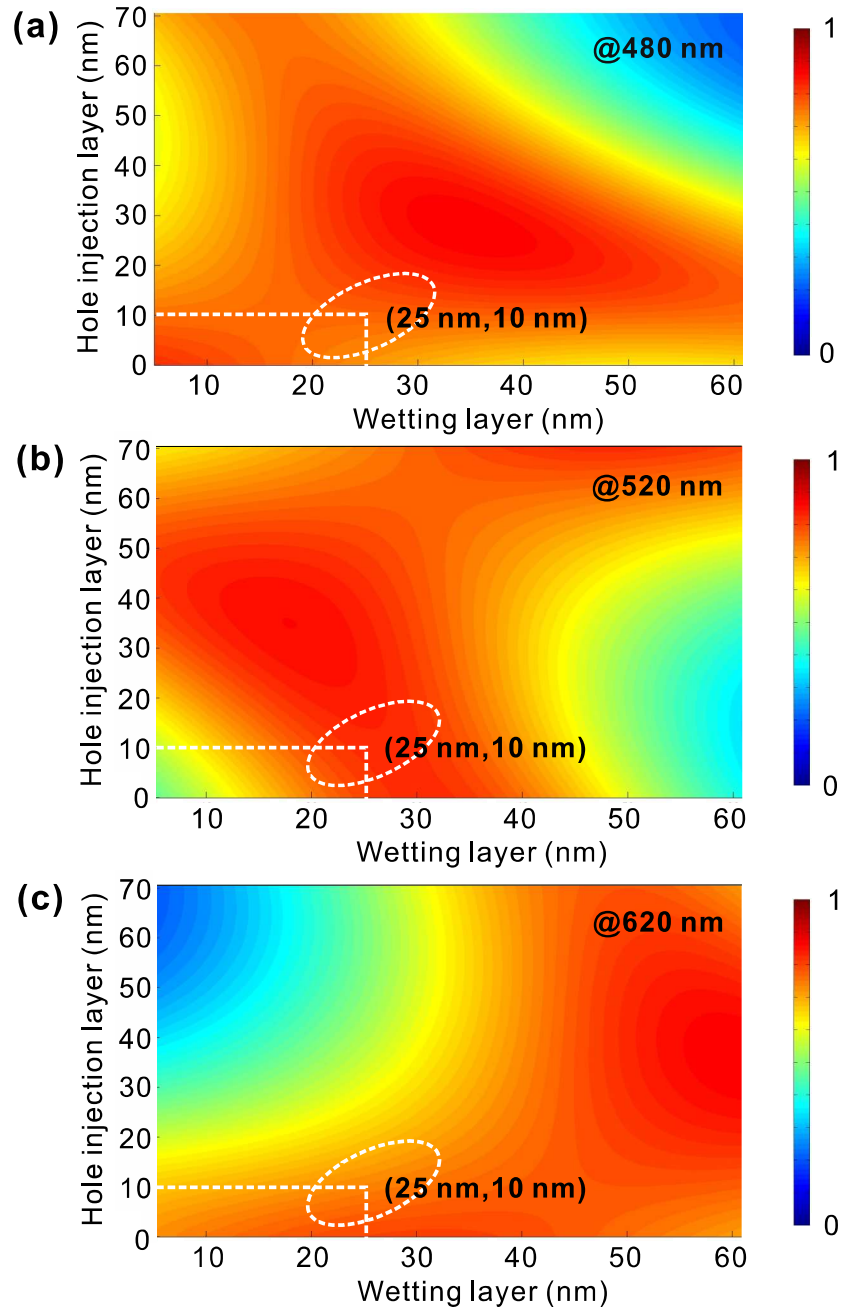


**Figure S3.** Two dimensional contour plots of simulated transmittance of a planar  $\text{MoO}_3/\text{Ag:Ca}/\text{MoO}_3$  MDCE as a function of the thickness of both the  $\text{MoO}_3$  hole-injection and wetting layers. For white emission, the optimum  $\text{MoO}_3$  thicknesses of the hole-injection and wetting layers are 10 nm and 25 nm, respectively.

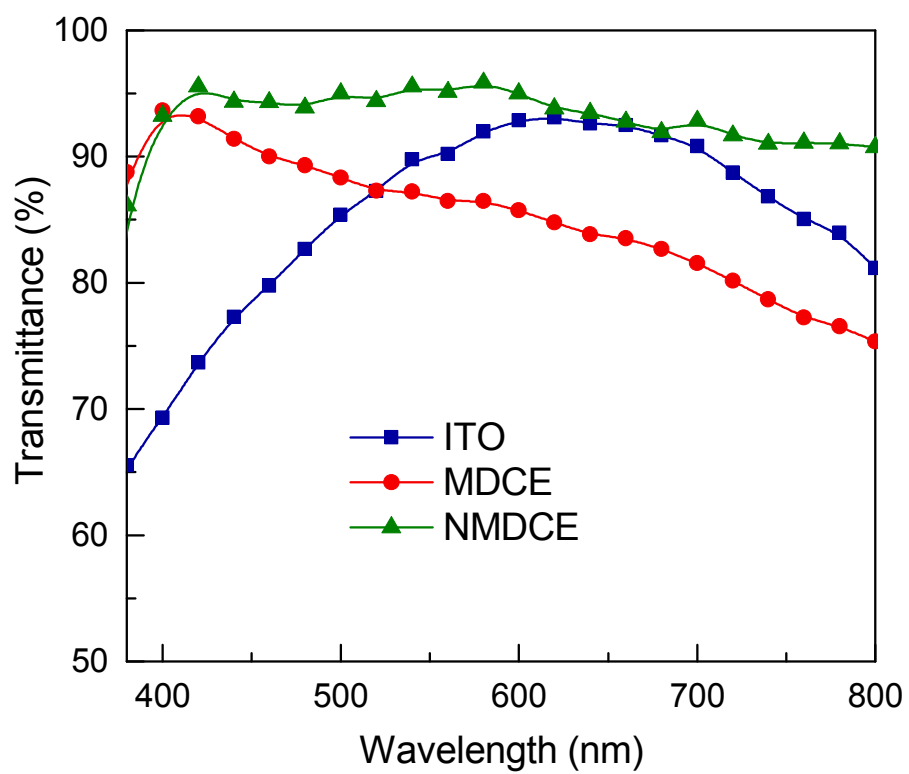


**Figure S4.** Transmittance spectra of bare transparent electrodes without plastic substrate.

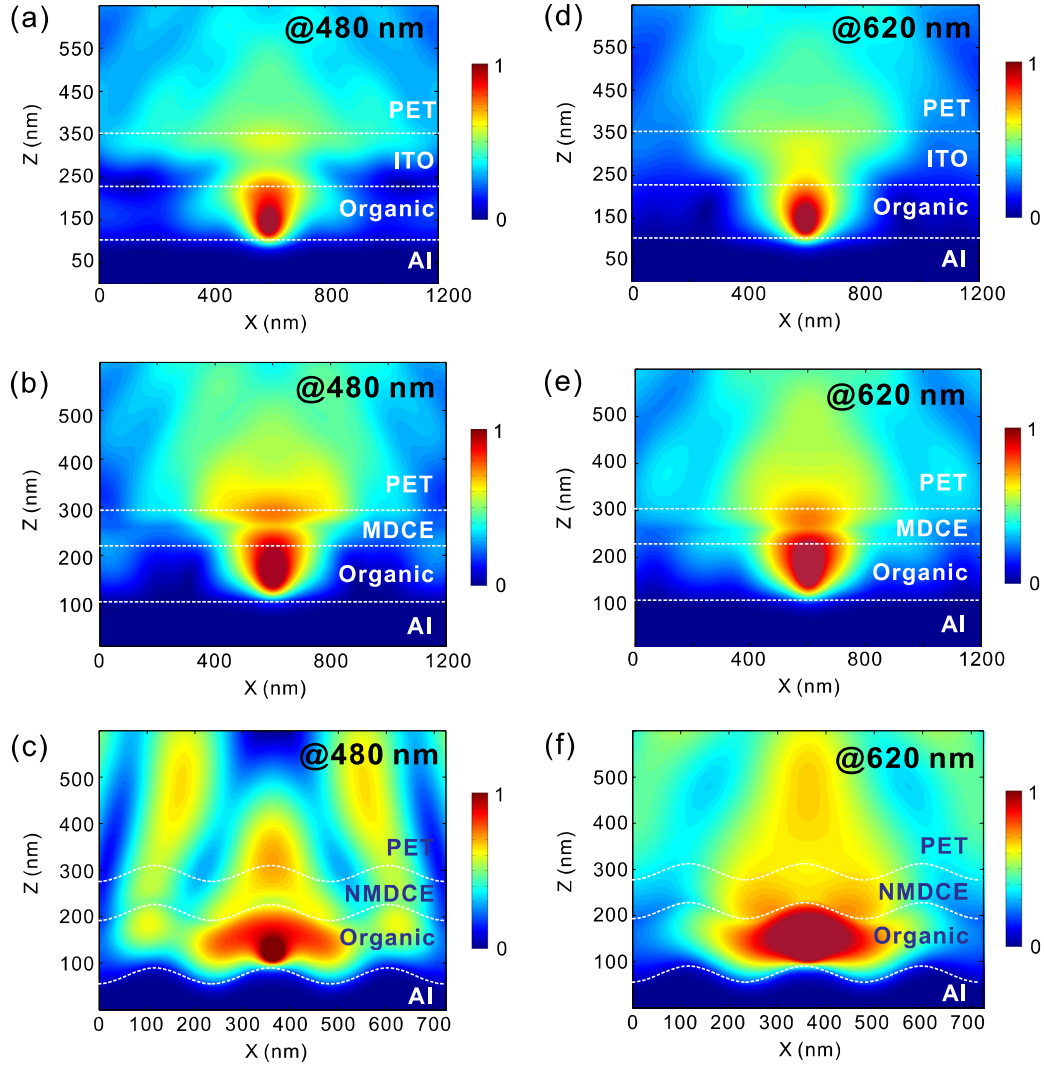


**Figure S5.** Normalized cross-section intensity field distributions in OLEDs on different electrodes using FDTD method (Rsoft FullWave). For propagation at 480 nm: (a) ITO, (b) MDCE and (c) NMDCE. For propagation at 620 nm: (d) ITO, (e) MDCE and (f) NMDCE.

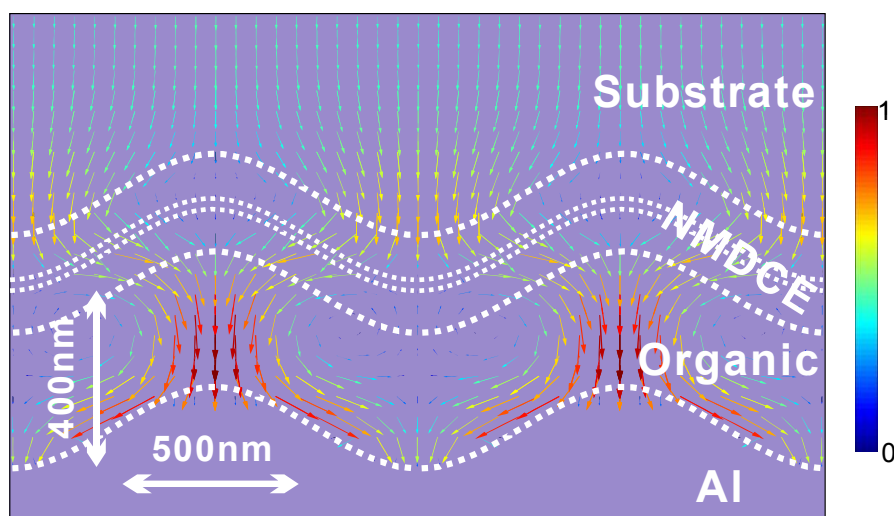


**Figure S6.** Energy flow diagram of the NMDCE device. Poynting vector distribution excited by a plane wave at 520 nm are calculated at incidence from substrate to device layers. The dashed lines represent the layer interface of different materials. The small arrows depict the flow direction of the energy flow and the colors stand for the relative intensity according to color bar. Bottom and top nanostructured metallic electrodes promote the photon flux collectively to propagate as an extraordinary optical vortex from the device to leaky modes eventually.

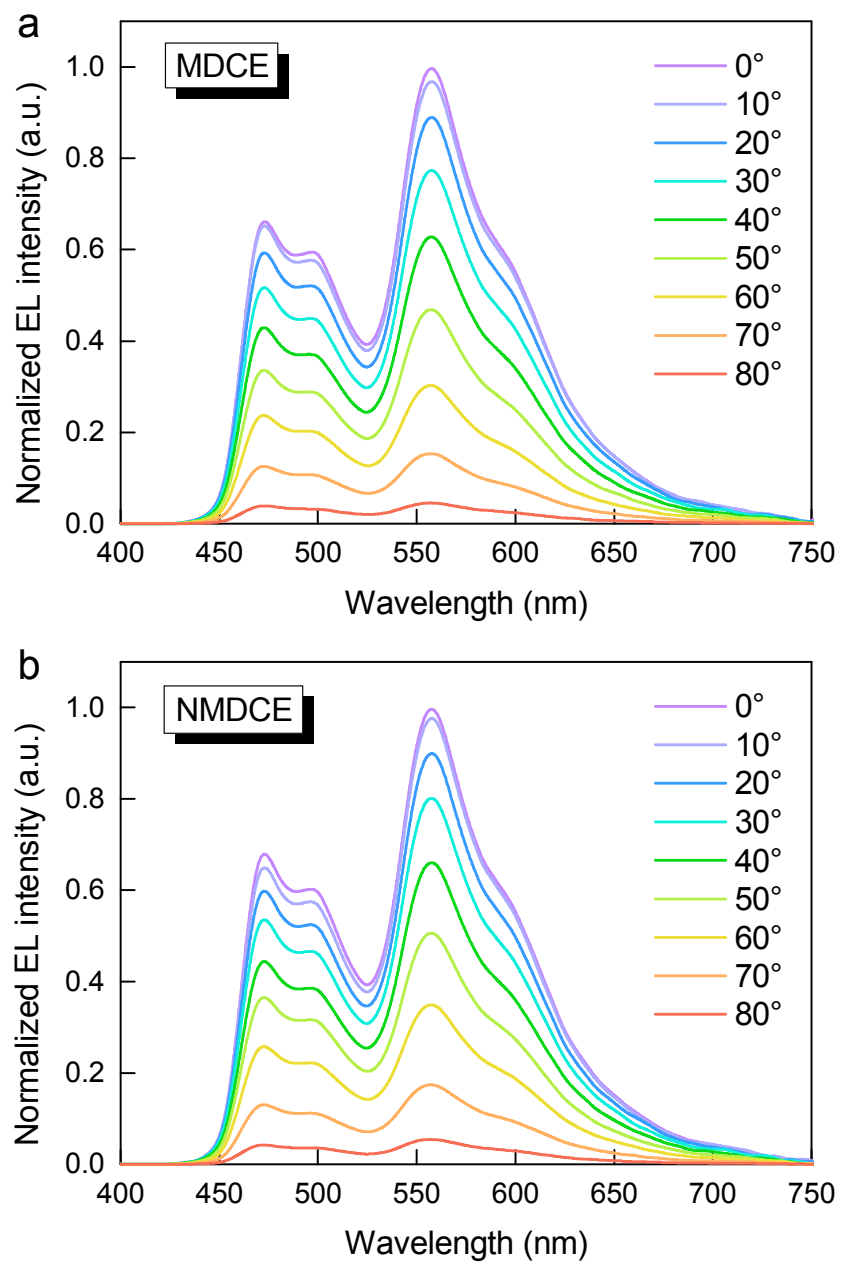


**Figure S7.** Angle dependence of emission spectra of white flexible OLEDs on (a) MDCE and (b) NMDCE.